

EVIDENCE FOR ABNORMAL H α VARIABILITY DURING NEAR-TRANSIT OBSERVATIONS OF HD 189733 B

P. WILSON CAULEY AND SETH REDFIELD

Wesleyan University

Astronomy Department, Van Vleck Observatory, 96 Foss Hill Dr., Middletown, CT 06459

ADAM G. JENSEN

University of Nebraska-Kearney

Department of Physics & Astronomy, 24011 11th Avenue, Kearney, NE 68849

ABSTRACT

Changes in levels of stellar activity can mimic absorption signatures in transmission spectra from circumplanetary material. The frequency and magnitude of these changes is thus important to understand in order to attribute any particular signal to the circumplanetary environment. We present short-cadence, high-resolution out-of-transit H α spectra for the hot Jupiter host HD 189733 in order to establish the frequency and magnitude of intrinsic stellar variations in the H α line core. We find that changes in the line core strength similar to those observed immediately pre- and post-transit in two independent data sets are uncommon. This suggests that the observed near-transit signatures are either due to absorbing circumplanetary material or occur preferentially in time very near planetary transits. In either case, the evidence for abnormal H α variability is strengthened, although the short-cadence out-of-transit data do not argue for circumplanetary absorption versus stellar activity caused by a star-planet interaction. Further out-of-transit monitoring at higher signal-to-noise would be useful to more strictly constrain the frequency of the near-transit changes in the H α line core.

1. INTRODUCTION

Much effort has been invested into understanding how stellar activity affects radial velocity measurements and broadband transit observations (e.g., Saar & Donahue 1997; Pont et al. 2011; Aigrain et al. 2012; Dumusque et al. 2014; Oshagh et al. 2014; Anderson & Korhonen 2015; Llama et al. 2015; Herrero et al. 2016; Hébrard et al. 2016; Chiavassa et al. 2017) and many studies exist of long-term activity variations, i.e. day to year timescales, for known exoplanet hosts (Boisse et al. 2009; Fares et al. 2010; Gomes da Silva et al. 2011, 2014; Figueira et al. 2016; Giguere et al. 2016). On the other hand, little investigation has been aimed at understanding stellar activity variations on very short timescales for known exoplanet host stars (i.e., minutes to hours). This is unsurprising as long-term variations play a more significant role in RV data sets collected sporadically across many nights. Similarly, even large variations in spectroscopic activity indicators (e.g., H α , Ca II, or Na I) are completely washed out in broadband photometric observa-

tions. With the increasing popularity of short-cadence, high-spectral resolution transit observations (e.g., Redfield et al. 2008; Jensen et al. 2012; Wyttenbach et al. 2015; Cauley et al. 2015, 2016; Barnes et al. 2016) it is important to understand the short-term behavior of host stars in order to differentiate between true absorption by planetary material and stochastic changes in stellar activity indicators potentially caused by star-planet interactions (SPIs).

In Cauley et al. (2015, 2016) we reported on pre- and post-transit H α absorption signatures in high-resolution data taken across two different transits of HD 189733 b. Similar signatures have been reported in atomic UV transitions for HD 189733 b (Ben-Jaffel & Ballester 2013; Bourrier et al. 2013) and WASP-12 b (Fossati et al. 2010; Haswell et al. 2012). Each of the H α signatures showed a different depth and time-series shape, suggesting that the physical mechanism is highly variable. Since absorption measurements from high-resolution transmission spectra are necessarily normalized relative to a reference spectrum, or a group of spectra, the absorption is by definition relative to another point in time. Thus if the reference spectrum is chosen during a time of higher

stellar activity, other spectra will show absorption, mimicking the loss of photons by line-of-sight material. The short baselines, i.e., a single night, for the high-cadence transit observations make it difficult to distinguish between these changes in the stellar activity level and true absorption by circumplanetary material.

In this paper we present out-of-transit observations of HD 189733 in order to further probe the frequency of the observed pre- and post-transit changes in the $H\alpha$ line core. Section 2 describes the observations and data reduction procedures. In Section 3 we present the $H\alpha$ time series data and discuss the statistical analysis of the changes in the $H\alpha$ signal. A brief summary is given in Section 4.

2. OBSERVATIONS AND DATA REDUCTION

Observations were performed using the Tull Coudé Spectrograph (Tull et al. 1995) on the Harlan J. Smith 2.7 meter telescope at McDonald Observatory. We collected data on five separate nights. A to-scale diagram of the phases during which the observations took place is shown in Figure 1. The night of 2016 July 29 was shortened due to persistent high humidity and 2016 September 19 was shortened because of heavy clouds during the first two hours of the night. The nights of 2016 July 31 and 2016 August 01 were shortened due to observatory functions requiring use of the telescope during the first third of each night. Details concerning the 2013 and 2015 Keck observations are presented in Cauley et al. (2015, 2016).

Spectra were taken with two different slits. We utilized the #5 slit for the first night of 2016 July 29 which has a width of $1.79''$ and resolving power of $R \sim 40,000$, or $\sim 7.5 \text{ km s}^{-1}$. These observations were typically 900 seconds in length. For the nights of 2016 July 30 and July 31 we used the #6 slit with $R \sim 30,000$ (or $\sim 10 \text{ km s}^{-1}$) and 600 second integrations in order to use a more similar cadence to the past Keck observations and to boost the signal to noise. Exposure times were increased to 900 s on 2016 August 01 due to moderate cirrus cloud coverage. The telluric standard HR 8634 was observed for approximately ten minutes each night. The spectra from 2016 July 29 were broadened to match the instrumental resolution of the observations taken with the #6 slit in order to standardize the data collected with different spectrograph settings.

Standard data reduction steps were taken, including bias subtraction, flat fielding with a median flat, and optimal extraction using custom IDL routines. Spectra were extracted for two separate orders, one containing the $H\alpha$ line and another containing a comparison Fe I line at 6677.98 \AA . The Fe I line is used as a control to ensure that the extraction and spectrum comparison procedures are not artificially producing signals in the

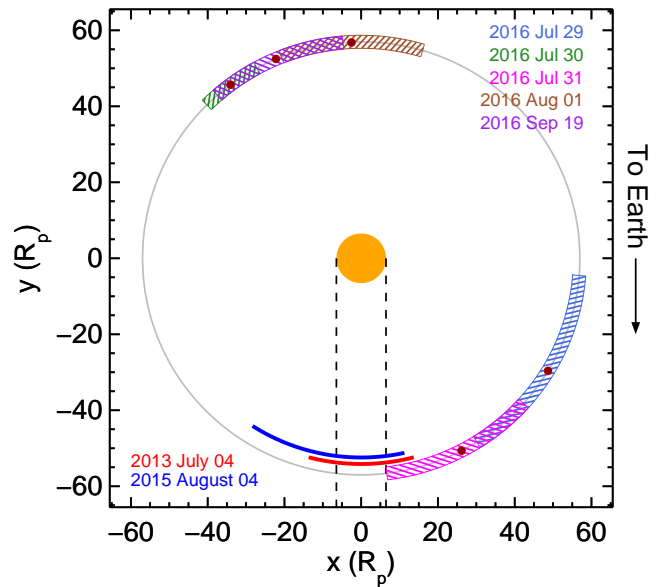


Figure 1. To-scale diagram showing the orbital phases during which the 2016 McDonald observations were performed (hatched regions) and the transit observations from Cauley et al. (2015, 2016) (solid red and blue lines). The in-transit portion of the orbit is marked with vertical dashed lines and the mean planet position during each set of 2016 observations is marked with a brown circle.

line cores. Wavelength solutions for the individual orders were found using Th-Ar lamp exposures and 3rd or 4th degree polynomial fits. Typically ~ 20 - 30 Th-Ar lines were used in the solution. Small wavelength shifts between individual spectra are corrected using strong stellar lines in the same order besides the line of interest. Each wavelength solution is then corrected for the barycentric velocity and HD 189733 system radial velocity, which we take to be -2.23 km s^{-1} (Di Gloria et al. 2015).

The telluric spectrum in the $H\alpha$ order was modeled using the program Molecfit (Kausch et al. 2014). We modeled the telluric spectrum in the Fe I order but it is very weak and results in negligible changes to the transmission spectrum. We first remove the blaze function and the broad stellar $H\alpha$ line from the telluric standard spectrum using a high order spline. Molecfit then fits the normalized telluric spectrum for the H_2O and O_2 column densities, as well as the instrumental resolution. This master telluric model is then scaled, shifted, and divided out of the individual observations.

The mean normalized $H\alpha$ spectrum from each night is shown in the top row of Figure 2. We also show the ratio of the master spectrum from each night compared with the master spectrum from 2016 September 19 in the middle row (see Equation 1). The middle rightmost panel shows the 2016 September 19 spectrum compared with the 2013 and 2015 master spectra. The equivalent width measurement $W_{H\alpha}$ (see Equation 2) for the $F_i/F_{\text{Sep19}} - 1$ spectra are given in the bottom left of the

middle panels, where negative $W_{H\alpha}$ indicates a deeper $H\alpha$ core relative to 2016 September 19, i.e., less core emission. The night-to-night $W_{H\alpha}$ values can be compared to the intra-night changes shown in Figure 4 and Figure 7. We also show histograms of the transmission spectra for $50 \text{ km s}^{-1} < |v| < 200 \text{ km s}^{-1}$ in the bottom panels. The same comparison for the Fe I control line is shown in Figure 3.

3. $H\alpha$ TIME SERIES ANALYSIS

Figure 2 shows that all of the July nights exhibit less $H\alpha$ core emission than the 2016 September 19 observations, suggesting that HD 189733 was in a more active state, or the visible hemisphere was more active, during the night of 2016 September 19. There is some fluctuation between the July nights with 2016 July 30 showing the most core emission and 2016 July 29 and 2016 August 01 showing the least. The 2013 data shows a similar activity level to 2016 July 30 while the 2015 data shows a much more active state than any of the other dates, with $\sim 10\%$ more $H\alpha$ core emission when compared with 2016 August 01. In a forthcoming paper, we note that the 2015 observations are over-active compared to the other examined nights from that study. The additional data presented here strengthens the conclusion that HD 189733 was especially active at that time.

In order to produce a time series of the relative changes in the $H\alpha$ core within an individual night, we produce a “transmission” spectrum that is identical to the definition of S_T from Cauley et al. (2015, 2016):

$$S_T = \frac{F_i}{F_{comp}} - 1 \quad (1)$$

where F_i is a single observation and F_{comp} is the master comparison spectrum constructed from the three highest signal-to-noise spectra from each night. We then calculate the equivalent width of the individual transmission spectra according to

$$W_{H\alpha} = \sum_{v=-200}^{+200} \left(1 - \frac{F_v}{F_v^{comp}} \right) \Delta\lambda_v \text{ \AA} \quad (2)$$

where F_v is the flux in the spectrum of interest at velocity v , F_v^{comp} is the flux in the comparison spectrum at velocity v , and $\Delta\lambda_v$ is the wavelength difference at velocity v . Uncertainties in $W_{H\alpha}$ are calculated by summing the transmission spectrum flux errors in quadrature across the same velocity range.

The phase-folded $H\alpha$ time series for all nights is shown in Figure 4 and the Fe I time series is shown in Figure 5. A histogram comparison of $W_{H\alpha}$ between the 2016 dates and the combination of the 2013 and 2015 dates is shown in Figure 6. The out-of-transit points from the 2013 and 2015 data sets are also shown in Figure 4. The magni-

tude of the pre-transit signals measured in Cauley et al. (2015, 2016) are marked with red and blue solid horizontal lines. It is clear that no changes in the out-of-transit monitoring data are of comparable strength to the 2013 pre-transit signal. Some changes, however, are of similar magnitude to the pre-transit absorption signals from 2015 presented in Cauley et al. (2016). The left panel of Figure 6 demonstrates that the 2016 $W_{H\alpha}$ measurements are consistent with the random measurement errors and show no significant deviations from zero. The right panel of Figure 6 shows that there is no correlation between $W_{H\alpha}$ and W_{FeI} , suggesting that the extraction and transmission spectrum procedures are not significantly contributing to the measurements. The same $W_{H\alpha}$ data is shown in Figure 7 but as a function of time from the midpoint of each set of observations.

To quantify the differences in the measured $W_{H\alpha}$ time series, we have calculated the absolute deviation from the median, or the ADM, for each night:

$$ADM = |W_{H\alpha}^i - \text{Median}(W_{H\alpha})| \text{ \AA} \quad (3)$$

where $W_{H\alpha}^i$ are the individual observations and $\text{Median}(W_{H\alpha})$ is the median of all observations. The empirical distribution function (EDF) of the ADM for each night is shown in the left panel of Figure 8. The right panel of Figure 8 shows the total EDFs for the 2016 data (green line) and the 2013 data combined with the 2015 data (magenta line). We also include normal and uniform distributions, generated using the 2016 data, for reference. We do not make any statistical comparisons using only the 2013 data due to the smaller number of observations compared with the 2015 data set. The 2013 and 2015 EDFs are plotted with dashed red and blue lines, respectively, in the left panel. Also shown in the left panel of Figure 8 are the two sided Kolmogorov-Smirnov (KS) statistic D_{KS} and the probability p_{KS} that the null hypothesis is true, i.e., that each EDF is drawn from the same parent distribution, for the individual 2016 EDFs compared with the 2015 EDF. The KS statistics are shown in the right panel for the comparison between both total EDFs.

For our purposes the EDF of the absolute deviation from the median highlights differences between a time series with structure, such as the 2015 data, and the apparently random deviations of a time series like those from the 2016 nights. Figure 8 shows significant differences between the 2015 EDF and the 2016 EDFs: the 2015 EDF flattens off near $ADM \sim 0.0025$ and then begins to increase again near $ADM \sim 0.0045$. In comparison, all of the 2016 EDFs are $\sim 80\%$ comprised of $ADM \lesssim 0.004$. These differences are born out in the KS statistics: with the exception of the 2016 Jul 29 observations, which contain only eleven data points, all of

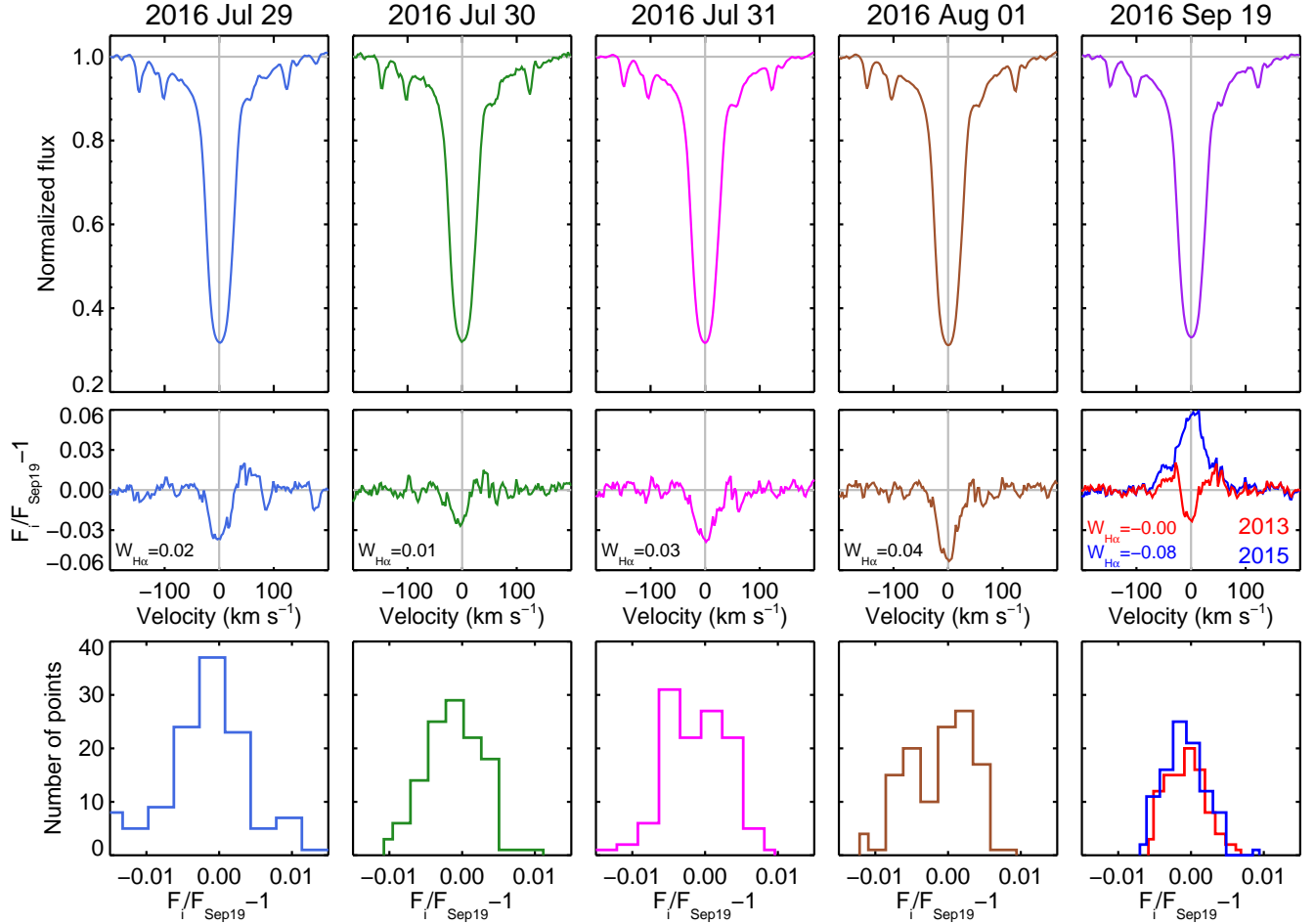


Figure 2. Average $H\alpha$ spectra for each night (top panel) and the “transmission” spectrum (see Equation 1) relative to 2016 September 19 (middle panels). The spikes near ~ 90 and 190 km s^{-1} in the 2016 July 29 S_T spectrum are telluric residuals. The equivalent width of the ratio spectrum, $W_{H\alpha}$ (also see Equation 2), is given in the middle panels. All of the July nights show less core emission than 2016 September 19, suggesting that HD 189733 was in a more active state during the 2016 September 19 observations. The 2015 $H\alpha$ core (bottom right panel) was strongly filled in relative to the 2016 observations, confirming the high activity state noted in Cauley et al. (2016). The bottom panels show histograms of the transmission spectrum for $50 \text{ km s}^{-1} < |v| < 200 \text{ km s}^{-1}$. The mild departure from purely Gaussian noise in the transmission spectra can be attributed to imperfect telluric subtraction.

the EDFs differ from the 2015 EDF at the 95% level, i.e., $P_{KS} < 0.05$. We can rule out the null hypothesis even more strongly ($> 99\%$) for the combined EDF test. This can be interpreted as the 2016 dates all showing random deviations from the median activity level while the 2015 data has distinct, sustained features that force data points contained in these features to be far from the median. This contributes to the EDF at the higher ADM values.

The significant differences between the out-of-transit 2016 monitoring and the very near-transit data suggest that something interesting is happening immediately before and after HD 189733 b transits. There are two possibilities: 1. the near-transit features are due to absorbing circumplanetary material; or 2. the stellar activity level, as measured in $H\alpha$, is experiencing abnormal changes *preferentially* at near-transit times. Using the current data it is not clear which of these two cases is

true. However, we can say with some confidence that *abnormal changes in the stellar activity level occur more frequently very close to planetary transits*. In addition, the nominal stellar activity level is much higher for the 2015 data compared with the 2013 data set, and the 2013 data shows a similar activity level to the 2016 observations, yet both the 2013 and 2015 observations show significantly different ADM distributions compared with the 2016 data. Thus we cannot attribute the abnormal near-transit $W_{H\alpha}$ measurements to high levels of stellar activity. Taken together, we believe this is strong evidence in support of SPIs or absorption by circumplanetary material in the HD 189733 system (Cuntz et al. 2000; Shkolnik et al. 2008; Shkolnik 2013; Strugarek et al. 2014; Miller et al. 2015; Pillitteri et al. 2015).

Finally, we note that if the $H\alpha$ variations are the result of SPIs near transit, the affected region on the star must be very near the sub-stellar point. We speculate

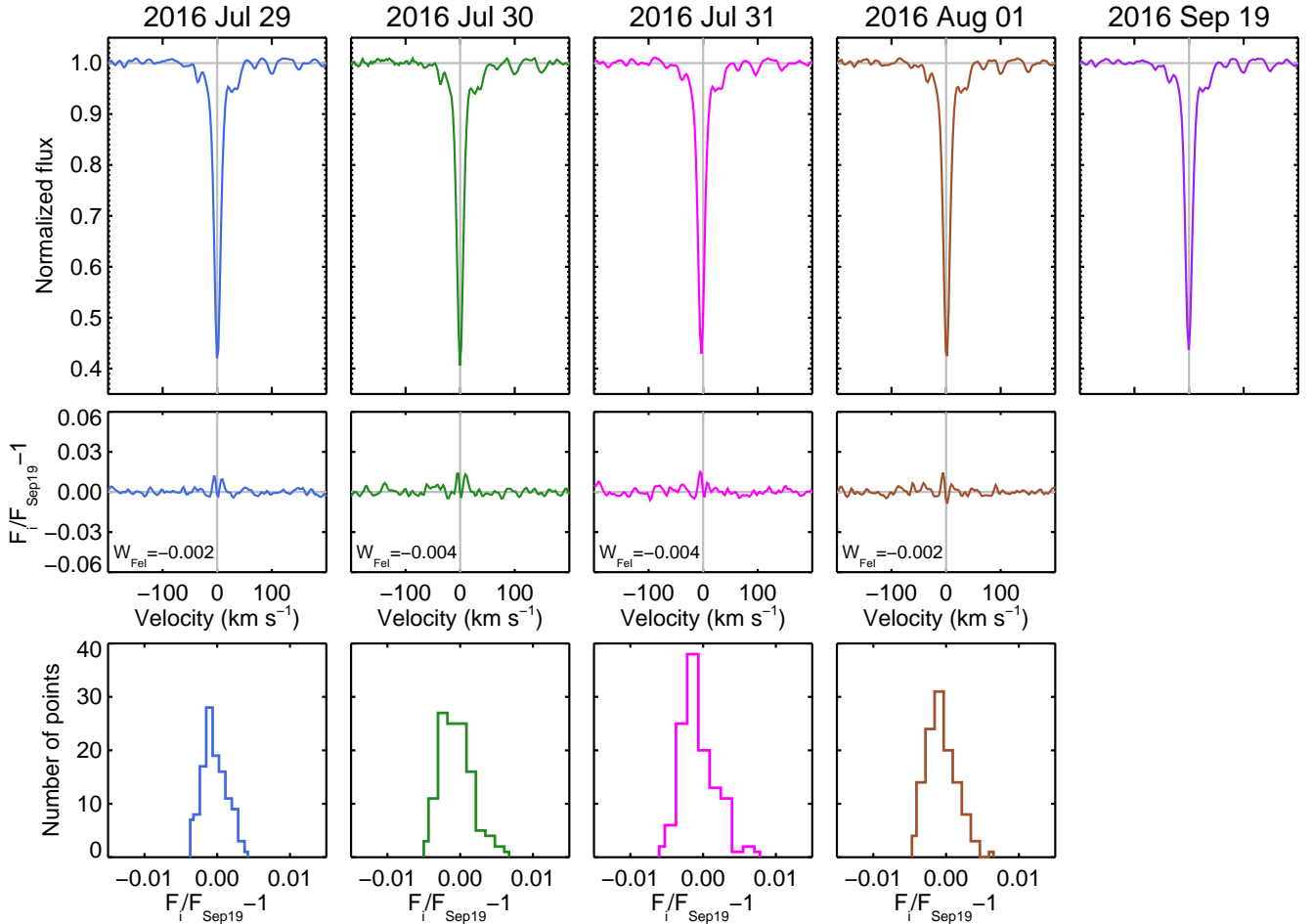


Figure 3. Same as Figure 2 but for the Fe I 6677.98 Å control line. The Fe I line is less sensitive to changes in stellar activity levels and the observed differences compared to the 2016 September 19 spectrum are negligible.

that this is evidence for the circumplanetary absorption interpretation since there is nothing special about the transit in the SPI interpretation. We leave this suggestion to further investigation.

4. SUMMARY AND CONCLUSIONS

We have presented new out-of-transit, high-cadence H α monitoring of HD 189733 over the course of 5 nights using the Tull Coudé spectrograph on the 2.7 meter Harlan J. Smith telescope at McDonald Observatory with the goal of establishing the frequency of changes in the stellar activity level at a similar magnitude to what we presented in Cauley et al. (2015, 2016). We do not find any variations in the H α core flux similar to what was observed immediately pre-transit in Cauley et al. (2015). With the exception of the 2016 July 30 data set, which only contains 11 observations, we find statistically significant differences between each of the out-of-transit nights and the out-of-transit signal from Cauley et al. (2016). This conclusion is strengthened when the combined out-of-transit data set is compared with the

combined near-transit observations. Our results suggest that changes in H α similar to those from Cauley et al. (2015) and Cauley et al. (2016) occur infrequently when the planet is far from transit. This is evidence for attributing the pre-transit signals to either absorbing circumplanetary material or some type of magnetic or tidal SPI near the sub-planetary point on the stellar surface. Further monitoring is necessary to understand the frequency and physical nature of the near-transit changes.

Acknowledgments: The authors thank the referee for their suggestions, which helped to significantly improve this manuscript. This paper includes data taken at The McDonald Observatory of The University of Texas at Austin. P. W. C. is grateful to Dave Doss and Brian Roman for their instrumental knowledge and observational support. This work was completed with support from the National Science Foundation through Astronomy and Astrophysics Research Grant AST-1313268 (PI: S.R.). A. G. J. is supported by NASA Exoplanet Research Program grant 14-XRP14 2-0090 to the University of Nebraska-Kearney. This work

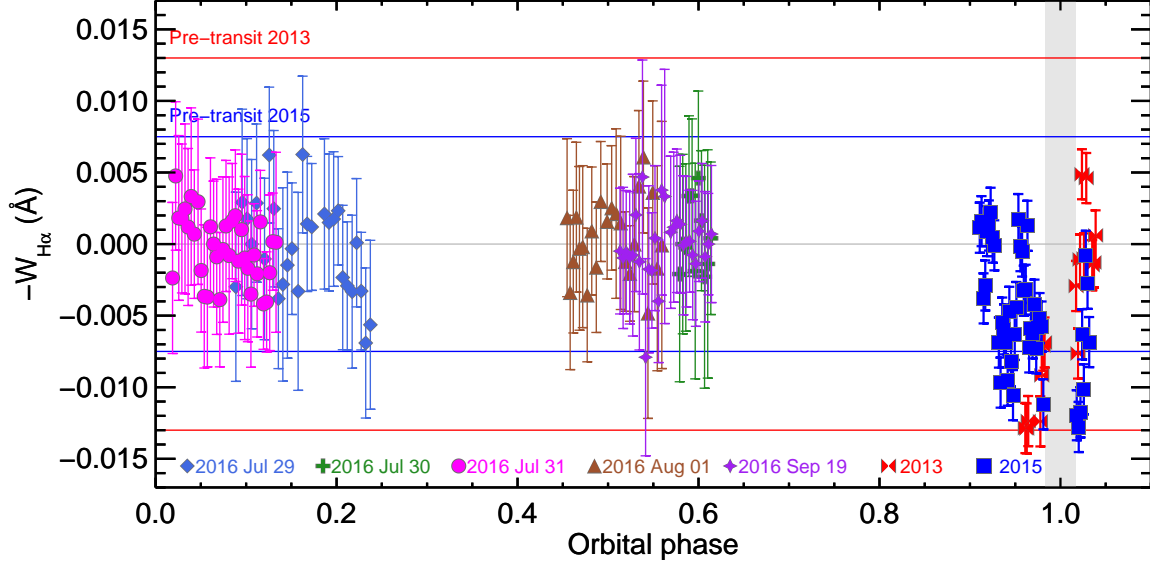


Figure 4. Phase-folded $W_{H\alpha}$ data from all nights. The horizontal red and blue lines indicate the magnitude of the pre-transit signals measured in the 2013 and 2015 data, respectively, from [Cauley et al. \(2015, 2016\)](#). The 2013 and 2015 data sets are shown in red bowties and blue squares, respectively, near phase ~ 0.95 . The transit is marked by the shaded gray region. Error bars represent 1σ uncertainties derived by adding the normalized flux errors in quadrature. No changes in $W_{H\alpha}$ are seen similar in magnitude to the 2013 pre-transit signal. Some sporadic changes similar to the level of 2015 pre-transit absorption are seen but their duration is typically much shorter.

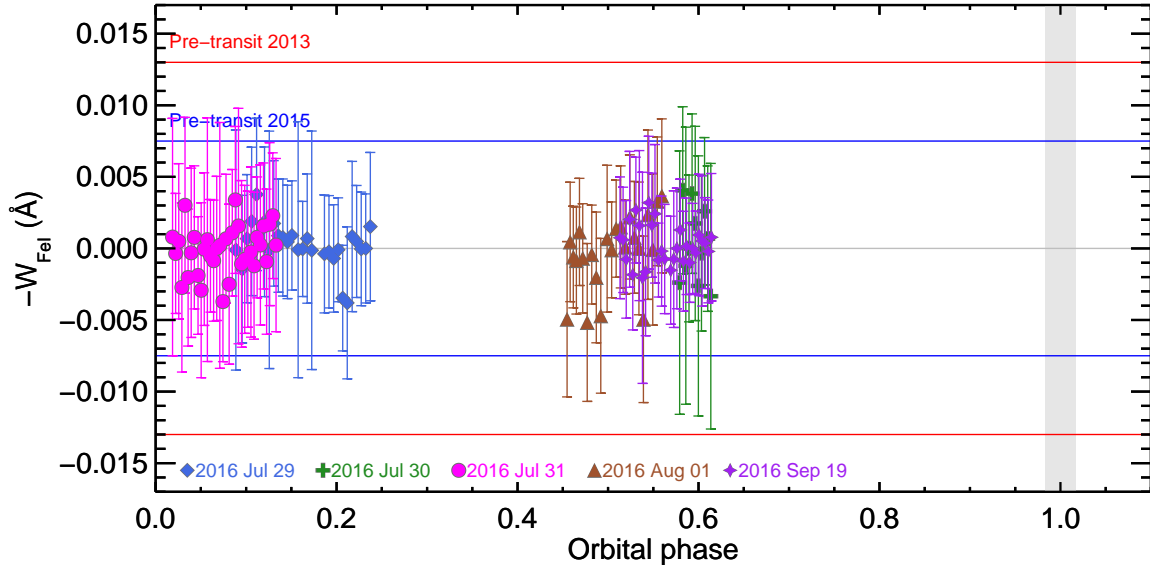


Figure 5. Same as [Figure 4](#) but for the Fe I control line. There is less scatter in the Fe I measurements due to the higher signal to noise in the order and the weak telluric spectrum. Measurements of the Fe I line are not available from the 2013 and 2015 data sets.

has made use of NASA’s Astrophysics Data System.

REFERENCES

- Aigrain, S., Pont, F., & Zucker, S. 2012, *MNRAS*, 419, 3147
 Andersen, J. M., & Korhonen, H. 2015, *MNRAS*, 3053, 3069
 Anglada-Escude, G., Amado, P. J., Barnes, J., et al. 2016, *Nature*, 536, 437
 Barnes, J. R., Haswell, C. A., Staab, D., & Anglada-Escudé, G. 2016, *MNRAS*, 462, 1012
 Ben-Jaffel, L., & Ballester, G. E. 2013, *A&A*, 553, A52
 Boisse, I., Moutou, C., Vidal-Madjar, A., et al. 2009, *A&A*, 495, 959
 Bourrier, V., Lecavelier des Etangs, A., Dupuy, H., et al. 2013, *A&A*, 551, A63

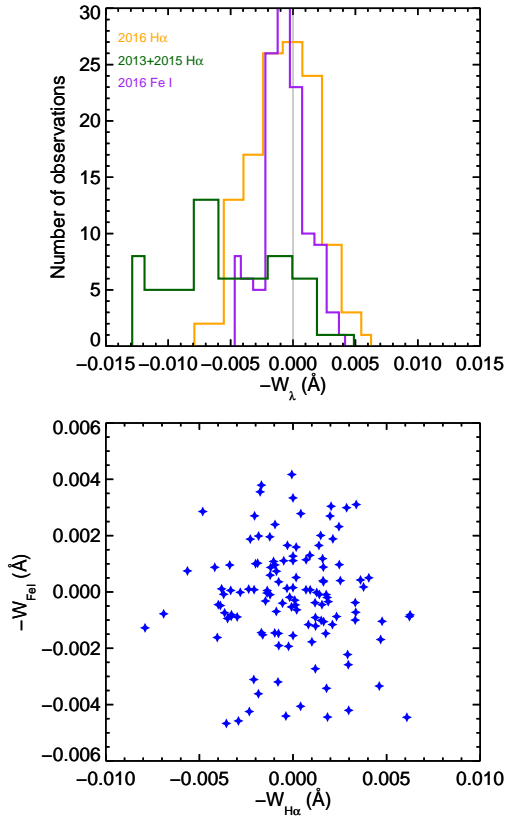


Figure 6. Histogram comparison (top panel) of the 2016 out-of-transit $W_{H\alpha}$ measurements (orange line) and the combined 2013 and 2015 near-transit measurements (dark green line). The Fe I control line measurements are also shown (purple line). The 2016 data for both $H\alpha$ and Fe I are approximately normal, with the $H\alpha$ distribution having mean ~ 0 and FWHM ~ 0.008 , suggesting there is no significant signal in the timeseries. The 2013+2015 distribution shows no identifiable structure. The bottom panel shows $W_{H\alpha}$ plotted against W_{FeI} . There is no correlation between the measurements, suggesting that systematics related to the extraction and transmission spectrum procedures are not contributing to the measured changes in $W_{H\alpha}$.

Cauley, P. W., Redfield, S., Jensen, A. G., et al. 2015, *ApJ*, 810, 13

Cauley, P. W., Redfield, S., Jensen, A. G., & Barman, T. 2016, *AJ*, 152, 20

- Chiavassa, A., Caldas, A., Selsis, F., et al. 2017, *A&A*, 597, A94
- Cuntz, M., Saar, S. H., & Musielak, Z. E. 2000, *ApJ*, 533, L151
- Di Gloria, E., Snellen, I. A. G., & Albrecht, S. 2015, *A&A*, 580, A84
- Dumusque, X., Boisse, I., & Santos, N. C. 2014, *ApJ*, 796, 132
- Fares, R., Donati, J.-F., Moutou, C., et al. 2010, *MNRAS*, 406, 409
- Figueira, P., Santerne, A., Suárez, M. A., et al. 2016, *A&A*, 592, 143
- Fossati, L., Haswell, C. A., Froning, C. S., et al. 2010, *ApJ*, 714, L222
- Giguere, M. J., Fischer, D. A., Zhang, C. X. Y., et al. 2016, *ApJ*, 824, 150
- Gomes da Silva, J., Santos, N. C., Bonfils, X., et al. 2011, *A&A*, 534, 30
- Gomes da Silva, J., Santos, N. C., Boisse, I., Dumusque, X., & Lovis, C. 2014, *A&A*, 566, 66
- Haswell, C. A., Fossati, L., Ayres, T., et al. 2012, *ApJ*, 760, 79
- Hébrard, É. M., Donati, J.-F., Delfosse, X., et al. 2016, *MNRAS*, 461, 1465
- Herrero, E., Ribas, I., Jordi, C., Morales, J. C., Perger, M., & Rosich, A. 2016, *A&A*, 586, A131
- Jensen, A. G., Redfield, S., & Endl, M., et al. 2012, *ApJ*, 751, 86
- Kausch, W., Noll, S., Smette, A., et al. 2014, *ASPC*, 485, 403
- Llama, J., & Shkolnik, E. L. 2015, *ApJ*, 802, 41
- Miller, B. P., Gallo, E., Wright, J. T., & Pearson, E. G. 2015, *ApJ*, 799, 163
- Oshagh, M., Santos, N. C., Ehrenreich, D., et al. 2014, *A&A*, 568, A99
- Pillitteri, I., Maggio, A., Micela, G., et al. 2015, *ApJ*, 805, 52
- Pont, F., Aigrain, S., & Zucker, S. 2011, *MNRAS*, 411, 1953
- Rajpaul, V., Aigrain, S., Osborne, M. A., Reece, S., & Roberts, S. 2015, *MNRAS*, 452, 2269
- Redfield, S., Endl, M., Cochran, W. D., & Koesterke, L. 2008, *ApJ*, 673, L87
- Saar, S. H., & Donahue, R. A. 1997, *ApJ*, 485, 319
- Shkolnik, E., Bohlender, D. A., Walker, G. A. H., & Collier Cameron, A. 2008, *ApJ*, 676, 628
- Shkolnik, E. L. 2013, *ApJ*, 766, 9
- Strugarek, A., Brun, A. S., Matt, S. P., & Réville, V. 2014, *ApJ*, 795, 86
- Tull, R. G., MacQueen, P. J., Sneden, C., & Lambert, D. L. 1995, *PASP*, 107, 251
- Wytttenbach, A., Ehrenreich, D., Lovis, C., Udry, S., & Pepe, F. 2015, *A&A*, 577, A62

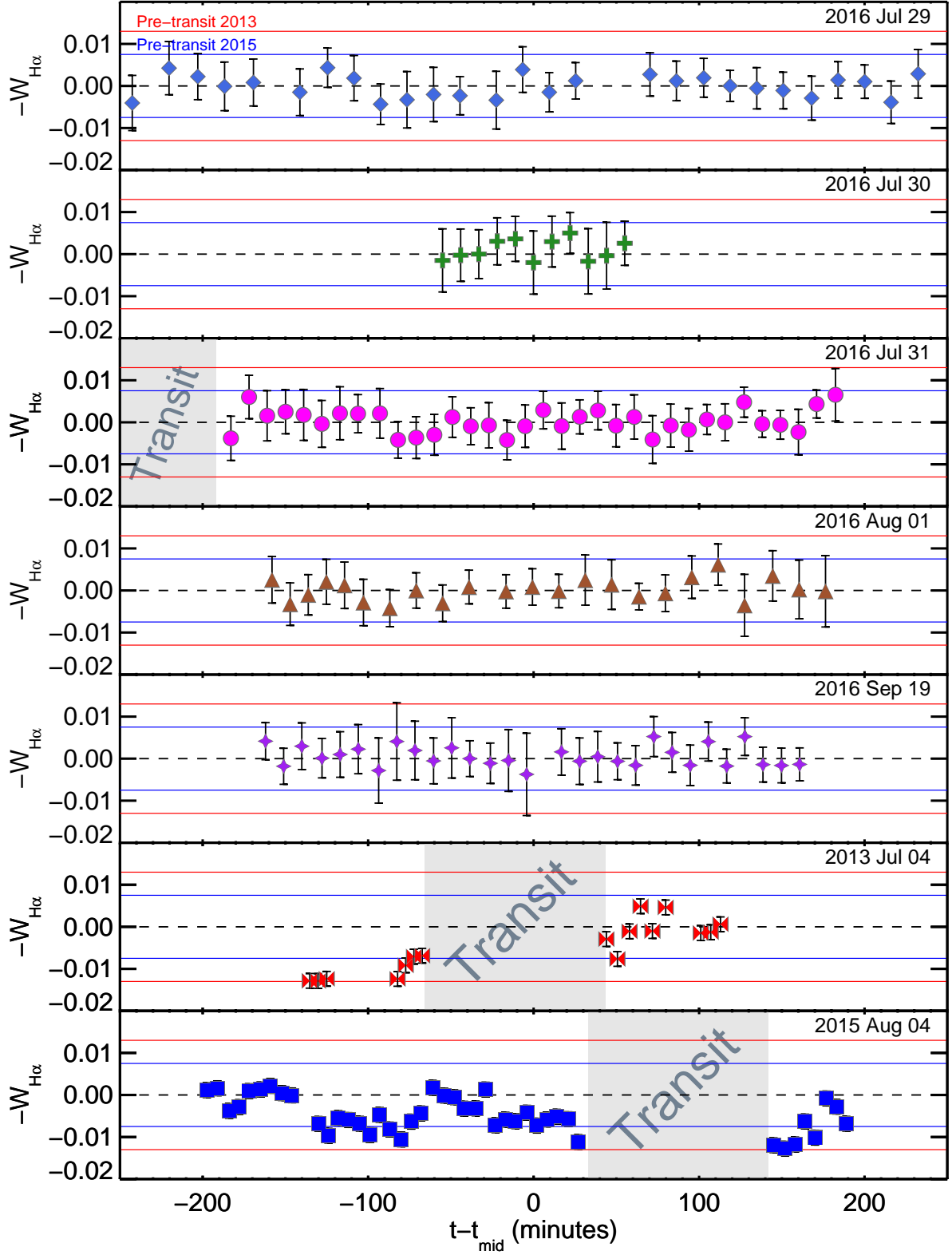


Figure 7. $W_{H\alpha}$ plotted as a function of time from the midpoint ($t - t_{mid}$) of each set of observations. Colors and symbols are the same as Figure 4. All nights are plotted on the same vertical and horizontal scale. Again, no changes in $W_{H\alpha}$ similar to the 2013 pre-transit change are seen in any of the time series. Some variations similar to the 2015 pre-transit change are seen but their duration is shorter and more erratic than the two dips seen in the 2015 data.

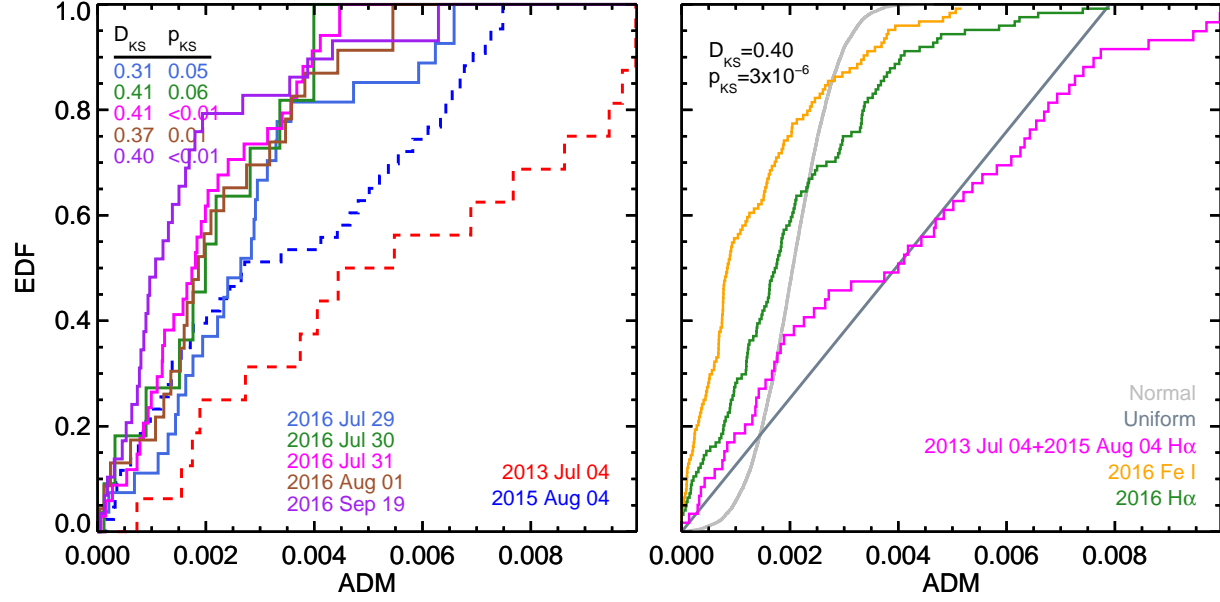


Figure 8. Left panel: Empirical distribution functions (EDF) for the ADM of each time series compared with the EDFs from the 2013 (red dashed line) and 2015 (blue dashed line) out-of-transit data. With the exception of July 30, all of the EDFs differ from the 2015 EDF at the $\geq 95\%$ level according to the two sided KS test. The KS statistics are shown in the upper left of the figure. Right panel: Total EDFs for all 2016 H α observations (green line) and the combined 2013 and 2015 H α data (magenta line). The Fe I EDF is also shown (orange line), which is very similar in structure compared with the 2016 H α EDF but scaled to lower values of the ADM. Uniform and normal distributions for the 2016 H α observations are shown for reference. The combined EDFs differ at the $> 99\%$ level, providing strong statistical evidence that the near-transit observation differ significantly from the far-from-transit observations in 2016.